Plasticization and Antiplasticization in Polycarbonates: The Role of Diluent Motion

P. Bergquist, Y. Zhu, A. A. Jones,* and P. T. Inglefield

Carlson School of Chemistry, Clark University, Worcester, Massachusetts 01610

Received February 10, 1998; Revised Manuscript Received May 17, 1999

ABSTRACT: A phosphorus-31 solid echo chemical shift anisotropy line shape study of tris(2-ethylhexyl) phosphate in tetramethyl polycarbonate determined the rate and amplitude of diluent motion in this mixed glass as a function of temperature and concentration. The dynamics of the diluent are observed to be bimodal with diluent in contact with other diluent on a random basis, displaying much greater mobility than diluent surrounded by polymer. A lattice model adequately accounts for the population of each type of diluent. The diluent in contact with other diluent considered to be a microcluster undergoes isotropic Brownian rotational diffusion with an apparent activation energy of 56 kJ/mol. The isolated diluent molecules undergo Brownian rotation restricted to a cone, and the rate and amplitude of this motion increase slowly with temperature. The temperature and breadth of the mechanical loss peak at a frequency of 1 Hz associated with rotation of the diluent in microclusters can be calculated from the interpretation of the line shape data. It is predicted to occur at a temperature of −56 °C, which lies on the low-temperature side of the polymer loss peak and may account for some of the increased mechanical loss peak at lower temperatures upon addition of diluent. The mechanical loss peak is little changed in amplitude upon addition of diluent, in contrast to significant suppression observed in bisphenol A polycarbonate. The coupling model of Ngai and Yee accounts for this difference in terms of the inherent rate of the sub-glass transition motion of the two polymers relative to the inherent rate of the motion of the diluent. The size of the microclusters was determined from proton spin diffusion to be 12 Å and to contain about two diluent molecules, in agreement with the lattice model description.

Introduction

The effect of diluent molecules on the mechanical properties of glassy polycarbonates has been studied by a number of techniques[1−13] including NMR in the past decade. Among these studies, NMR is especially useful since the motion of the polymer and the motion of the diluent can be monitored separately through a combination of isotopic labeling and selection of nuclei for study.

This contribution is an extension of some of the earlier studies where ^{31}P line shapes have been used to study the motion of a phosphate ester in bisphenol A polycarbonate (BPA-PC) and in a blend of poly(styrene) and poly(phenylene oxide).[6−13] One-dimensional solid echo phosphorus-31 chemical shift anisotropy line shapes are an effective means of determining the rate and amplitude of ester motion. This and similar diluents modify the modulus of the glassy polymer, and the motions observed by NMR can be related to changes in the sub-glass transition mechanical loss of the material. Two changes in mechanical response can accompany the addition of a diluent. First, the low-temperature loss peak of BPA-PC can be suppressed[10,12] raising the modulus, which is often referred to as antiplasticization. However, as diluent concentration is increased, a new loss peak can appear associated with the rotation of some diluent molecules below the glass transition.[8,12] This leads to a reduction of modulus, and the two effects compete with each other.

In this report, the motion of tris(2-ethylhexyl) phosphate (TOP) is studied in a polycarbonate where the phenylene rings are disubstituted with methyl groups adjacent to the carbonate unit (TMBPA-PC). The structures of the two components of the mixed glass considered for study here are given in Figure 1. In this polycarbonate, the glass transition temperature increases

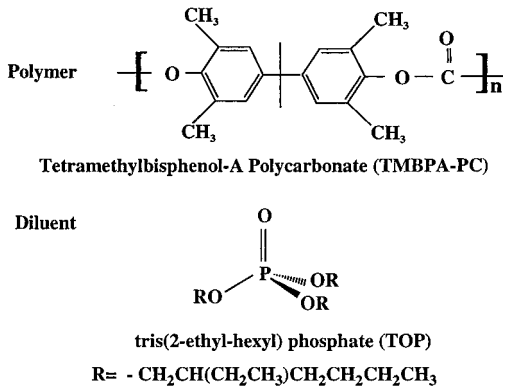

Figure 1. Structures and abbreviations of diluent and polymer.

by 50 deg and the low-temperature loss temperature increases by 150−170 deg, both relative to BPA-PC.[14,15] These changes in the mechanical properties caused by the presence of the methyl groups on the phenylene rings are part of the motivation for this study. In BPA-PC the low-temperature loss peak is at −100 °C at a frequency of 1 Hz, and some of the TOP molecules are observed to rotate at about −60 °C in the mixed glass of these two materials.[12] The large shift of the low-temperature peak in going from BPA-PC to TMBPA-PC means diluent rotation will likely occur at a lower temperature than the low-temperature loss peak in the substituted polycarbonate. In both polycarbonates, the low-temperature loss peak is associated with π flips of the phenylene rings. Diluents are observed to suppress the flips in BPA-PC as seen by NMR[1,2] as well as through the reduction of intensity of the mechanical loss peak, and it is an interesting question to see whether the diluent has the same effect on TMBPA-PC. In this study, the temperature and con-

10.1021/ma980205g CCC: $18.00
Published on Web 10/27/1999

centration dependence of the diluent rotation will be established although no NMR experiment will be performed to observe the dynamics of the TMBPA-PC. Mechanical data are available in an accompanying paper to monitor the changes in the sub-glass transition relaxations.[16]

There are several recent models for describing the changes in mechanical response noted upon the addition of diluent to a polymer like polycarbonate. The most common approach to this kind of system is based on free volume considerations. Maeda and Paul[3−5] have suggested a simple calculation that yields free volume estimates which account for gas transport in a series of mixed glasses. Typically, the free volume goes through a minimum as the amount of diluent is added to the glassy polymer. A decrease in transport and mechanical loss would be expected over the concentration range where free volume decreases.

Fischer et al. proposed a free volume fluctuation model[1] in which sub-glass transition motions depend on the availability of local free volume fluctuations. The distribution of free volume fluctuations is altered by the addition of a diluent, and if high free volume fluctuations are reduced, then local chain motions leading to sub-glass transition motions would also be reduced.

A lattice model[6−13] has also been proposed that focuses on the local surroundings of either the polymer or the diluent to infer the extent of molecular level mobility in the glass. In this model, if the diluent molecule is surrounded by polymer, the diluent molecule will not become rotationally mobile until the glass transition is reached. Diluent molecules that are in contact with other diluent molecules are more mobile, and depending on the intrinsic mobility of the diluent, these microclusters can begin to undergo rotation below the thermal glass transition temperature and can be a source of mechanical loss leading to a reduction in modulus. The level of diluent−diluent contact increases as diluent concentration is raised, and this is associated with the softening of mixed glasses as the concentration of diluent is raised. The number of diluent−diluent contacts is calculated from a lattice model assuming a random distribution of polymer repeat units and diluent molecules on the lattice.

A reduction in local polymer mobility is considered to occur in the lattice model as a result of reduced local free volume by the addition of a single isolated diluent molecule next to a chain repeat unit. This is based on a consideration of local free volume fluctuations much like Fischer's model,[1] but only the first diluent molecule next to a polymer unit is assumed to improve local packing and reduce free volume. This reduction leads to antiplasticization but only at low diluent concentrations. The lattice model focuses on the local environment because this is the length scale most important to NMR observations, and such observations led to the proposal of this approach.

The last model is a coupling model developed by Ngai and Yee.[16,17] This model interprets relaxation behavior in terms of dynamics and constraints on dynamics. If a diluent molecule is added to a polymer and the diluent is intrinsically less mobile than the sub-glass transition process present in the polymer, the coupling of motion between the less mobile diluent and the more mobile polymer motion leads to a reduction in polymer motion and thus antiplasticization. The coupling shifts the relaxation times to longer times, increases the breadth of the distribution of relaxation times, and raises the apparent activation energy. Interestingly for the system to be studied here, if the diluent motion is intrinsically more mobile than the sub-glass transition process in the polymer, then addition of diluent should speed up the relaxation of the polymer instead of slow it down or suppress it even at low diluent concentrations.

A difference between the lattice model and the other models is associated with the distribution of relaxation times.[6−13] The lattice model proposes distinct relaxation time distributions depending on the local surroundings of the unit in question. This leads to relaxation processes that are bimodal or involve two distributions centered at different times. A diluent molecule surrounded by polymer is observed to have far less mobility than diluent molecules in contact with other diluent molecules. Similarly, polymer units in contact with a diluent microcluster are observed to be sufficiently more mobile that for instance a new distinct $T_{1\rho}$ minimum[10] occurs instead of simply a broadening of the distribution.

Proton spin diffusion[13] has been used to measure the size of the microclusters proposed in the lattice model, and indeed the clusters contain two or three molecules at a diluent concentration of 10 wt % or so. The basis of the protons spin diffusion measurements is the Goldman−Shen[18] sequence which distinguishes spatial regions based on mobility differences and is therefore ideal for measuring the size of mobile domains in a mixed glass.

Experimental Section

Samples of four concentrations (5, 10, 15, and 20 wt %) of TOP in TMBPA-PC were prepared by Xiao et al.[16] These materials were optically clear films which were packed and sealed in NMR tubes.

^{31}P NMR powder spectra were taken on a Bruker MSL300 spectrometer operating at a frequency of 121 MHz. The ^{31}P $\pi/2$ pulse width was 5 μs. Spectra were recorded using a Hahn echo pulse sequence preceded by cross-polarization and with proton decoupling. Echo delay times of 5, 10, 50, 100, and 200 μs were used, and both the intensity and shape of the line were monitored.

The 10 wt % sample of TOP in TMBPA-PC was studied by proton spin diffusion. The experiments were performed on a modified Bruker SXP spectrometer operating at a proton frequency of 90 MHz. Phase cycling was used to minimize spin−lattice relaxation effects.[19] A typical proton spectrum consist of a narrow Lorentzian line superimposed on a broader Gaussian line as has been observed in a related system.[13] In the Goldman−Shen experiment discrimination times of 50 μs were employed, and free induction decays were acquired after mix times ranging from 0.03 to 80 ms. At short mix times, the free induction decay consists of the narrow Lorentzian component, and as the mix time is lengthened, the broader Gaussian component grows back at the expense of the Lorentzian component.

Results and Interpretation

The ^{31}P Hahn echo spectra at TOP concentrations of 5, 10, 15, and 20 wt % are the basis of the study of diluent dynamics, and representative spectra at a concentration of 15 wt % are given in Figure 2. The spectra at the other concentrations are deposited as Supporting Information. The general shapes of the lines as a function of temperature and concentration are qualitatively quite similar to those observed for TOP in BPA-PC.[12] Therefore, the same strategy for interpretation will be pursued: namely, the dynamics are assumed to be bimodal. TOP molecules in microclusters

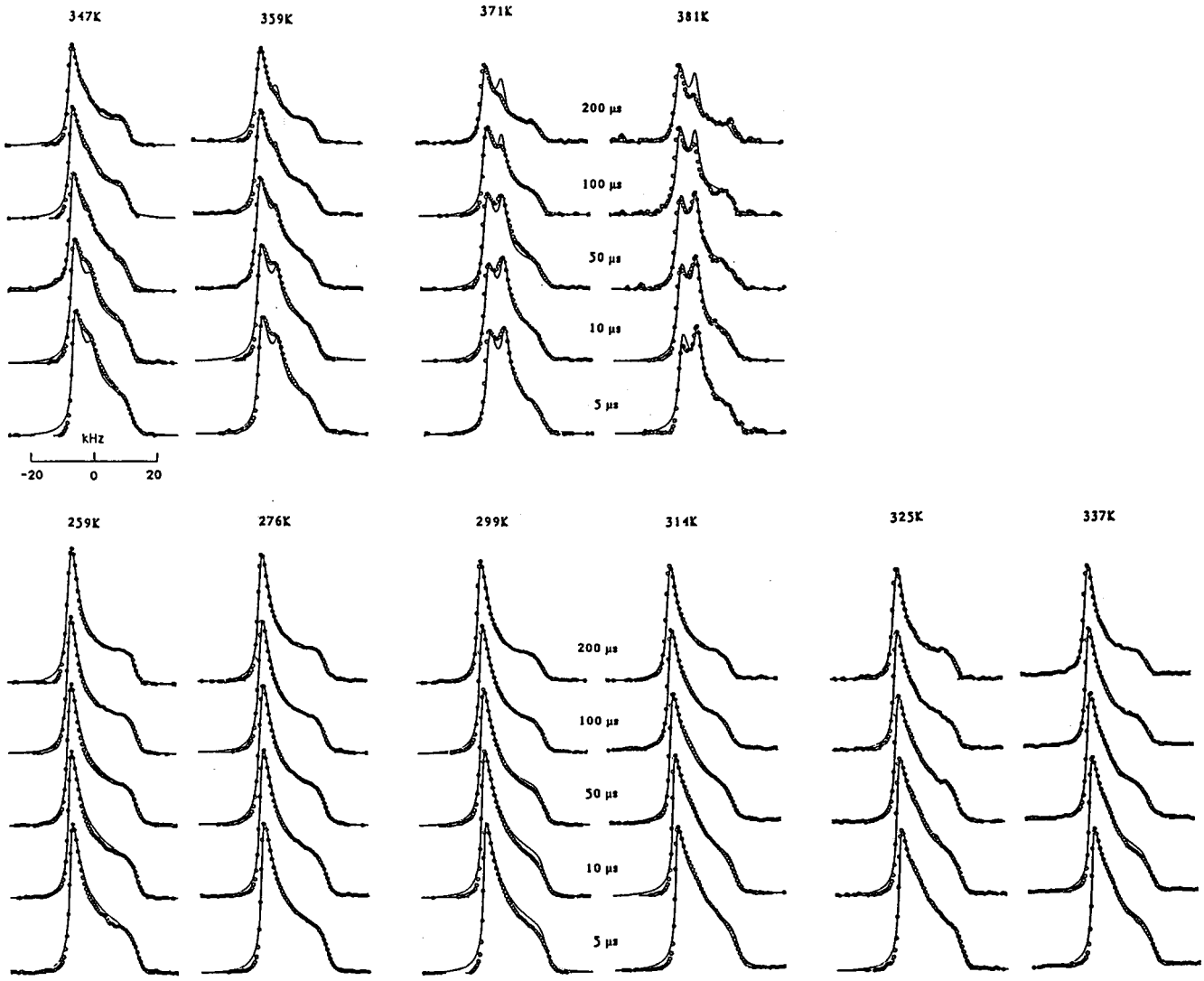

Figure 2. ^{31}P echo line shapes, experimental data in circles and simulations as lines, for 15% TOP at different echo delays and different temperatures.

undergo Brownian rotational diffusion with a distribution of correlation times. Sillescu's rate matrix[20] is used to describe the rotational diffusion motion, and the Williams−Watts[21] stretched exponential correlation function written as a sum of exponentials is used to provide the distribution of correlation times. The TOP molecules surrounded by polymer units are best described as undergoing rotation restricted to a cone. These diluent molecules do not begin isotropic rotational diffusion until the thermal glass transition is reached. The cone angle is allowed to grow with temperature below the glass transition, and the rate of this librational type of motion is allowed a weak temperature dependence that is essentially linear with the square root of temperature. The calculation of the echo line shape follows the approach given by Wittebort.[22] The specifics of the mathematics for each of these aspects have been presented before.[12]

The motional parameters used to simulate the echo line shapes include a rate, population, and amplitude for the restricted motion as well as a rate and a breadth parameter (the fractional exponent of the Williams−Watts) for the fast component. Table 1 contains a listing of the slow component rate, population, and cone angle amplitude for each concentration and temperature. The fast component rate at all temperatures and concentrations is given by an apparent activation energy of 56 kJ/mol and an Arrhenius prefactor of 3.7×10^{-14} with a breadth parameter $\alpha = 0.7$. Figure 2 displays the experimental spectra as points superimposed on the simulated spectra shown as a line.

The simulation includes matching the reduction factor, *R*, which is the integrated intensity of the solid echo relative to that of the free induction decay. The main reduction of intensity occurs when the time scale of the motion is comparable to the echo delay times, and a comparison of experimental and simulated reduction factors can be made from Figure 2 where absolute relative intensity is presented. The motional description entered into the Wittebort formalism yields both a simulated line shape and a simulated reduction factor.[12]

For each of the concentrations about 50 spectra are acquired and simulated. At the higher temperatures and concentrations, the largest deviations between simulations and observations occur at the longest delay time. Of the 209 spectra acquired for all concentrations, about five differ beyond experimental error. These deviations are mostly associated with a more rapid reduction of the fast component with increasing echo delay time than is predicted by the simulation. The fast component of all four concentrations is fit with the same rate parameters (activation energy and Arrhenius prefactor). A

Table 1. Fitting Parameters for the ^{31}P NMR Hahn Echo Spectra (Theoretical LB = 1200)

temp (K)	slow component rate (s^{-1})	slow component population (%)	cone angle	reduction factor at 200 μs simulation	reduction factor at 200 μs expt
		5% TOP			
259	1.131×10^3	100	25	0.81	0.86
276	1.138×10^3	100	28	0.76	0.81
299	1.150×10^3	100	30	0.78	0.82
314	1.155×10^3	100	30	0.78	0.86
325	1.160×10^3	100	30	0.78	0.86
337	1.165×10^3	100	30	0.78	0.81
347	1.171×10^3	100	33	0.72	0.79
359	1.172×10^3	100	33	0.72	0.76
371	1.180×10^3	100	33	0.72	0.79
381	1.190×10^3	100	35	0.69	0.74
393	1.195×103	98	40	0.64	0.73
		10% TOP			
259	1.131×10^3	100	25	0.81	0.89
276	1.138×10^3	100	28	0.76	0.78
299	1.150×10^3	100	30	0.78	0.84
314	1.155×10^3	100	30	0.78	0.73
325	1.160×10^3	96	33	0.69	0.75
337	1.165×10^3	96	33	0.69	0.69
347	1.171×10^3	96	35	0.67	0.67
359	1.172×10^3	96	35	0.67	0.59
371	1.180×10^3	90	40	0.63	0.60
381	1.190×10^3	86	40	0.65	0.68
393	1.195×10^3	78	40	0.67	0.69
		15% TOP			
259	1.131×10^3	98	25	0.80	0.79
276	1.138×10^3	95	28	0.73	0.70
299	1.150×10^3	95	33	0.68	0.72
314	1.155×10^3	90	33	0.65	0.70
325	1.160×10^3	90	35	0.62	0.65
337	1.165×10^3	90	35	0.63	0.70
347	1.171×10^3	82	35	0.62	0.63
359	1.172×10^3	76	35	0.63	0.60
371	1.180×10^3	65	40	0.62	0.59
381	1.190×10^3	64	40	0.66	0.57
		20% TOP			
259	1.21×10^3	81	25	0.68	0.69
276	1.25×10^3	81	28	0.64	0.59
299	1.30×10^3	81	35	0.58	0.64
314	1.33×10^3	75	35	0.55	0.52
325	1.35×10^3	66	35	0.51	0.51
337	1.36×10^3	61	35	0.52	0.56
343	1.37×10^3	58	35	0.53	0.53
347	1.38×10^3	58	35	0.55	0.54
359	1.39×10^3	49	40	0.57	0.58
367	1.40×10^3	44	40	0.61	0.59

slight adjustment of the parameters for the higher concentrations would improve the fit, but the number of parameters would increase. At the expense of a slight improvement in fit, it seems better to leave the rate of the fast component for all concentrations to be given by one activation energy and one Arrhenius prefactor. Note that these same two parameters also fit the fast component in 84 spectra reported[12] for TOP in BPA-PC.

A typical proton line shape for the sample is shown in Figure 3, which is again much like that obtained on the TOP in BPA-PC system.[13] As mentioned, the proton line shape consists of a broad Gaussian component and a superimposed narrow Lorentzian component. The Goldman−Shen (GS) experiment selects for the narrow component, and then as mix time lengthens, the broad component is repopulated. Figure 4 shows a series of free induction decays from a Goldman−Shen experiment at various mix times. Examination of Figure 4 shows the slow exponential decay at short mix times and the presence of both fast and slow decay components at longer mix times. The free induction decays, $G(t)$, are fit as a combination of a Lorentzian form and a Gaussian form.[13]

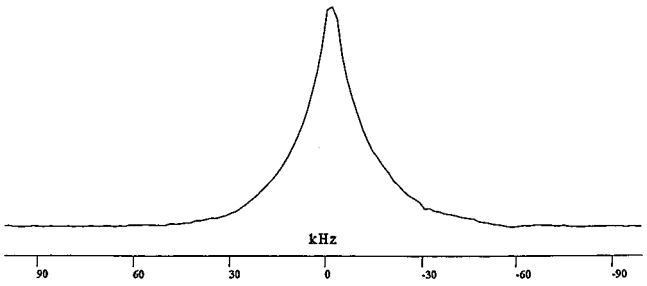

Figure 3. ^{1}H line shape for 10% TOP in TMBPA-PC at 339 K and a mixing time of 50 ms.

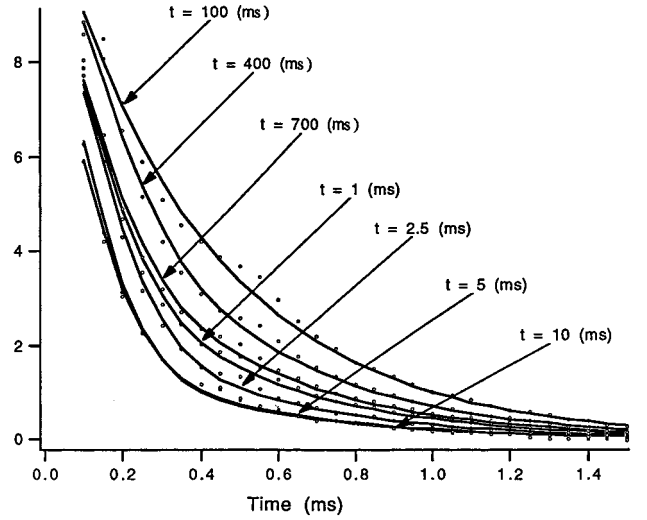

Figure 4. Free induction decays from a Goldman−Shen experiment at 339 K with a discrimination time of 50 μs and mixing times between 0.01 and 10 ms for 10% TOP in TMBPA-PC.

$$G(t) = Ae^{-(t/T_{2l})^2} + (1 - A)e^{-(t/T_{2m})} \quad (1)$$

The spin−spin relaxation time of the less mobile component in the GS experiment is T_{2l}, and a Gaussian form for the time dependence is assumed. The spin−spin relaxation of the more mobile component in the GS experiment is T_{2m}, and a time dependence corresponding to a Lorentzian is assumed. The quantity A is a function of mix time and is used to monitor the repopulation of the broad Gaussian component following the selection of the narrow component in the first part of the GS experiment. The recovery of the less mobile component in the GS experiment is monitored by the quantity $R(t_{mix})$ where

$$R(t_{mix}) = A(t_{mix})/A(\infty) \quad (2)$$

and $A(\infty)$ is the population of the less mobile Gaussian component at infinite time in the absence of any spin−lattice relaxation.

Expressions for the recovery factor as a function of mix time based on spin diffusion have been developed by Cheung and Gerstein.[23] The key parameters are the spin diffusion constant, D, and the domain size, b. The Cheung and Gerstein expression neglects spin−lattice relaxation and assumes a random distribution of more mobile domains in the sample. The three-dimensional form of the recovery equation best suited for the sample

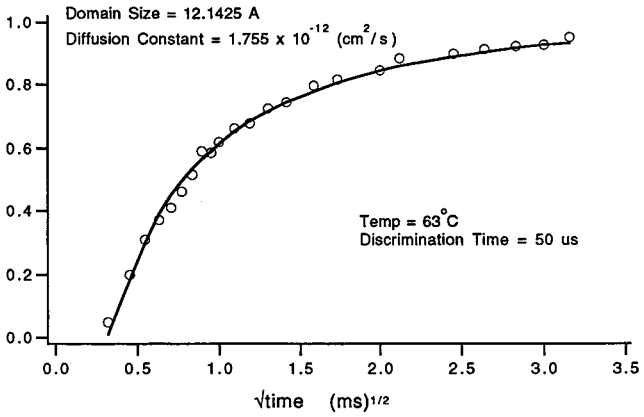

Figure 5. Recovery curve of the Goldman−Shen experiment.

Table 2. Parameters from Goldman−Shen Experiment for TMBPA-PC

temp (K)	t_0 (μs)	D/b^2 (3D) (ms^{-1})	$R(\infty)$	b (3D) (A)	D (10^{-12} cm^2 s^{-1})	T_{2m} (μs)	T_{21} (μs)
339	50	0.119	0.933	12.1	1.755	420	240

under consideration is

$$R(t) = 1 - \phi_x(t)\,\phi_y(t)\,\phi_z(t) \tag{3}$$

where each $\phi(t)$ has the form

$$\phi(t) = \exp(Dt/b^2)\,\mathrm{erfc}(Dt/b^2)^{1/2} \tag{4}$$

Figure 5 shows a typical recovery curve fit to eqs 3 and 4 which yields a value of 0.119 ms^{-1} for D/b^2. The recovery curve is offset from zero along the time axis. This generally indicates the presence of a finite interface between the two domains in a spin diffusion experiment.[23] An earlier extensive study of proton line shapes and proton spin diffusion on TOP in BPA-PC found that a number of polymer repeat units adjacent to the mobile diluent molecules are also more mobile than the polymer matrix in general. There is likely to be a gradual change from more mobile to less mobile polymer repeat units with distance from the mobile diluent molecules which could produce the apparent presence of an interface in the spin diffusion data.

To obtain a value for b as a measure of domain size, D will be estimated from the equation presented by Cheung and Gerstein,[23] where a is the average distance between adjacent protons in the less mobile domain. Somewhat arbitrarily, a is set at 1.8 Å, corresponding to the intramolecular separation of methyl and methylene protons. Given this choice for D, values of D and b are tabulated in Table 2 along with T_{2m} and T_{2l}.

Discussion

Visual inspection of Figure 2 indicates the TOP in TMBPA-PC is less mobile at the same temperature and concentration as TOP in BPA-PC.[12] This conclusion rests on the appearance of the narrower line at higher temperatures which appears on top of the usual tensor line shape. If the simulation parameters are considered, the change from BPA-PC to TMBPA-PC is associated with an decreased population of more mobile species. The rate of motion of the more mobile species is the same as in BPA-PC, and the amplitude of motion for the slow species is actually larger in TMBPA-PC. Figure 6 plots the population of more mobile species as a function of temperature for both polymer systems, and

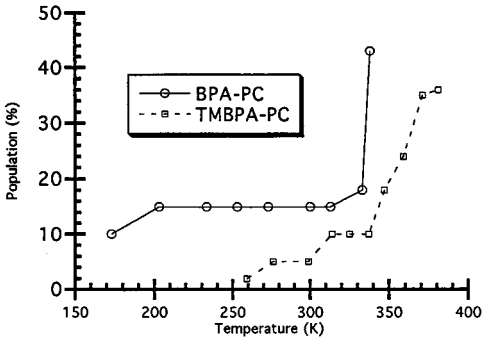

Figure 6. Population of the fast component versus temperature from the ^{31}P line shape simulations for 15% TOP in BPA-PC and TMBPA-PC.

Table 3. Glass Transition Temperatures of TOP in TMBPA-PC

concn (% TOP in TMBPA-PC)	T_g (K)	concn (% TOP in TMBPA-PC)	T_g (K)
0	476	15	388
5	441	20	371
10	415	100	139

at all temperatures the more mobile population is smaller in TMBPA-PC. If however the comparison is not made at the same temperature but rather at the same temperature relative to the glass transition, then the populations in the two polymers become closer and are almost the same just below T_g. In BPA-PC plus 15% w/w TOP the more mobile population is 45% while it is 36% in TMBPA-PC with the same concentration of TOP.

The fraction of more mobile diluent was reported earlier[8] for a series of polymer−diluent systems ar a concentration of 20 wt % diluent. For temperatures 5 deg below the glass transition, the population of mobile diluent varied from 55 to 65% while a value of 56% is reported here for 20 wt % TOP in TMBPA-PC. A detailed discussion of the lattice model predictions in that earlier study[8] led to values of 60 ± 5%, in fair agreement with the current result.

It is interesting to note that the rate of motion of the TOP molecules in the microclusters is the same in both TMBPA-PC and BPA-PC, and of course this yields the same activation energy of 56 kJ/mol. It would appear that dynamics in the microclusters is at best weakly coupled to the host matrix since both the glass transition motions and the sub-glass transition motions are the same.

On the other hand, the motion of the isolated diluent molecules, those completely surrounded by polymer, is quite different. These molecules do not rotate until the glass transition of the mixed glass is attained, and these T_g values are quite different as shown in Table 3. Furthermore, the amplitude of the motion of the isolated molecules also differs in the two systems, being considerably larger in TMBPA-PC as shown in Figure 7. This larger amplitude would appear to reflect the increased free volume of the TMBPA-PC polymer host which also has a lower density and a higher permeability.[24]

The mechanical responses of the two mixed glasses also differ. The position of the mechanical loss peak in temperature and frequency associated with rotation of the diluent molecules in microclusters can be calculated from the rate, breadth parameter, and apparent activation energy,[12] and it is exactly the same for the two systems. At an experimental frequency of 1 Hz it has a maximum at −56 °C. However, the observed mechanical

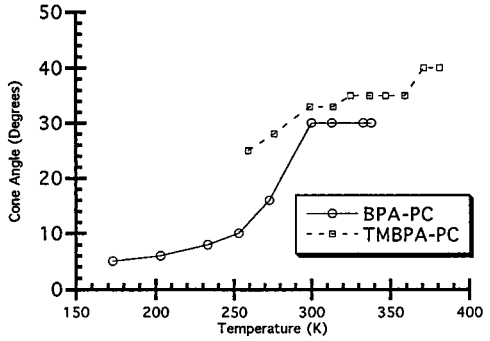

Figure 7. Cone angle versus temperature for 15% TOP in BPA-PC and TMBPA-PC.

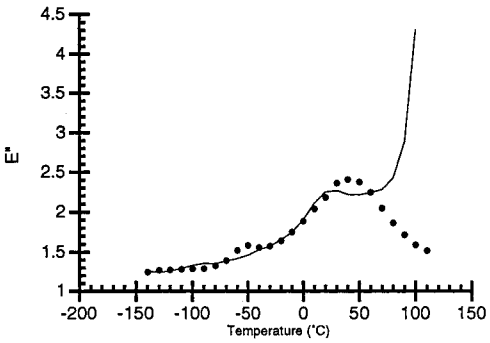

Figure 8. Mechanical loss peak (solid points) calculated form the NMR data and the low-temperature loss of pure TMBPA-PC drawn together with the experimental mechanical loss (solid line[16]) for system of TMBPA-PC plus 10% TOP.

response which depends on both polymer and diluent motion is distinctly different for the two systems. BPA-PC has a sub-glass transition maximum at −100 °C, and TMBPA-PC has a sub-glass transition maximum in the 50−70 °C range. Thus, the diluent motion occurs at a higher temperature than the sub-glass transition process in BPA-PC and at a lower temperature in the TMBPA-PC. In the mixed glass based on BPA-PC the mechanical response shows a decreasing loss peak which shifts to higher temperatures as diluent is added, and in the TMBPA-PC system there is rather little change in intensity of the loss peak but some increase of loss at lower temperatures. For BPA-PC there has been an NMR study of the motion of the polymer in the presence of another similar ester diluent, dibutyl phthalate,[10] and this shows a similar change of mechanical properties upon addition of diluent. In that case a fraction of the sub-glass transition process was shifted to high temperatures and indeed did not appear to take place until the glass transition. This aspect was related to classic antiplasticization behavior. A portion of the sub-glass transition process did remain in the same general temperature range, but it was shifted to slightly lower temperatures. Given this information, the apparent shift to higher temperatures of the mechanical loss of the mixed glass of TOP and BPA-PC was attributed to the presence of diluent rotation on the high-temperature side of the original loss peak and not just to a shift of the sub-glass transition motion of the polymer.[12]

For the TMBPA-PC case under consideration here, some increase in loss at lower temperatures would again be attributed to diluent motion. Figure 8 shows the position of the diluent loss peak calculated from the NMR data added to the loss peak of pure TMBPA-PC. The position and breadth of a loss peak can be calculated from the correlation times and activation energy determined from NMR, and this kind of calculated loss peak is combined with the mechanical response of pure TMBPA-PC taken from the literature.[12] The relative magnitudes of the two loss peaks are not known but were adjusted to give a calculated response that is as close to the observed response for 10% TOP in TMBPA-PC as possible. The motion of the diluent appears as a small loss peak on the low temperature side of the polymer gamma loss peak in the calculated response while the experimental spectrum shows only a extension of the main loss peak to lower temperatures. On the high temperature side of the experimental polymer gamma loss peak the glass transition is also seen as a sharp rise in loss which is not present in the calculated response since the pure TMBPA-PC response was used which has a much higher glass transition temperature relative to the mixed system. An important point with respect to the Ngai and Yee model is that the experimental loss peak occurs at a lower temperature than the calculate response which included diluent motion. Thus, from this comparison, one would conclude that the gamma loss peak in TMBPA-PC has moved to lower temperature as predicted by the Ngai and Yee model. It is important to remember that only the diluent motion was observed in this NMR study, and thus changes in the polymer motion cannot be predicted on the basis of the diluent dynamics measured here. Only an NMR study of the polymer motion itself in TMBPA-PC would definitively answer the question of any changes in the dynamics of the polymer associated with a change in the temperature of the polymer loss peak. Nevertheless, with the information that is available, it appears that the gamma peak in TMBPA-PC did move to lower temperature.

In the mechanical spectrum of the TOP/TMBPA-PC mixed glass there is also little suppression of the loss peak[16] compared to the significant intensity changes seen in the TOP/BPA-PC system. Here the lattice and free volume models have no simple prediction, but the coupling model predicts that if the diluent motion is intrinsically faster than the sub-glass transition process of the polymer, there will be no antiplasticization or suppression of the polymer motion.[17] Though the polymer motion has not been studied in the TMBPA-PC system by a method such as NMR which can follow the dynamics of the polymer alone, the prediction appears to be correct on the basis of the mechanical response.[16] It would certainly be worthwhile to examine a number of systems including NMR measurements of the polymer motion in this system to see whether the intrinsic time scale of the diluent motion relative to the polymer motion is the determining factor in the occurrence of antiplasticization.

The domain size of 12 Å measured for the diluent microclusters in TMBPA-PC is within experimental error of that obtained for the mixed glass based on BPA-PC.[13] In the latter case, the domain was found to contain about two diluent molecules, in good agreement with the lattice model predictions. The same outcome is found here so this structural aspect of the study is quite consistent between the two systems. A series of different polymers and diluents have now been considered, and the applicability of the lattice model in characterizing the structure and dynamics of the diluent in these polymers has carried through all systems.[6−13] All display bimodal diluent dynamics and microclusters

resulting from a random distribution of diluent molecules in the mixed glass system.

Acknowledgment. This research was carried out with the financial support of the National Science Foundation Grant DMR9303193. P.B. acknowledges support from ONR AASERT Grant N000149310994.

Supporting Information Available: Figures containing ^{31}P echo line shapes for 5, 10, 15, and 20% TOP at different echo delays and temperatures. This material is available free of charge via the Internet at http://pubs.acs.org.

References and Notes

(1) Fischer, E. W.; Hellman, G. P.; Spiess, H. W.; Horth, F. J.; Ecarius, U. Wherle, M. *Makromol. Chem. Suppl.* **1985**, *12*, 189.
(2) Wherle, M.; Hellman, G. P.; Spiess, H. W. *Colloid Polym. Sci.* **1987**, *265*, 815.
(3) Maeda, Y.; Paul, D. R. *J. Polym. Sci., Polym. Phys.* **1987**, *25*, 957.
(4) Maeda, Y.; Paul, D. R. *J. Polym. Sci., Polym. Phys.* **1987**, *25*, 981.
(5) Maeda, Y.; Paul, D. R. *J. Polym. Sci., Polym. Phys.* **1987**, *25*, 1005.
(6) Kambour, R. P.; Carbeck, J. D.; Nachlis, W. L. *J. Non-Cryst. Solids* **1991**, *131*−*133*, 563.
(7) Kambour, R. P.; Kelly, J. M.; McKinley, B. J.; Cauley, B. J.; Inglefield, P. T.; Jones, A. A. *Macromolecules* **1988**, *21*, 2937.
(8) Cauley, B. J.; Cipriani, C.; Ellis, K. Roy, A. K.; Jones, A. A.; Inglefield, P. T.; McKinley, B. J.; Kambour, R. P. *Macromolecules* **1991**, *24*, 403.
(9) Jones, A. A.; Inglefield, P. T.; Liu, Y.; Cauley, B.; Roy, A. K.; Kambour, R. P. *Mater. Res. Soc. Symp. Proc.* **1991**, *215*, 109.
(10) Liu, Y.; Roy, A. K.; Jones, A. A.; Inglefield, P. T.; Ogden, P. *Macromolecules* **1990**, *23*, 968.
(11) Jones, A. A.; Inglefield, P. T.; Liu, Y.; Roy, A. K.; Cauley, B. J. *J. Non-Cryst. Solids* **1991**, *131*−*133*, 556.
(12) Liu, Y.; Turnbull, M. M.; Jones, A. A.; Inglefield, P. T.; Kambour, R. P. *Solid State NMR* **1993**, *2* 289.
(13) Liu, Y.; Inglefield, P. T.; Jones, A. A.; Kambour, R. P. *Magn. Reson. Chem.* **1994**, *32*, 518.
(14) Yee, A. F.; Smith, S. A. *Macromolecules* **1981**, *14*, 54.
(15) Hansen, M. T.; Boeffel, C.; Spiess, H. W. *Colloid Polym. Sci.* **1993**, *271*, 446.
(16) Xiao, C.; Wu, J.; Yang, L.; Yee, A. F.; Xie, L.; Girdley, D.; Ngai, K. L. *Macromolecules* **1999**, *32*, 7913.
(17) Ngai, K. L.; Rendell, R. W.; Yee, A. F.; Plazek, D. J. *Macromolecules* **1991**, *24*, 61.
(18) Goldman, M.; Shen, L. *Phys. Rev.* **1966**, *144*, 321.
(19) Packer, K. J.; Pope, J. M. *J. Magn. Reson.* **1983**, *55*, 378.
(20) Sillescu, H. *J. Chem. Phys.* **1971**, *54*, 2110.
(21) Williams, G.; Watts, D. C. *Trans. Faraday Soc.* **1970**, *66*, 80.
(22) Wittebort, R. J.; Olejniczak, E. T.; Griffin, R. G. *J. Chem. Phys.* **1987**, *86*, 5411.
(23) Cheung, T. T. P.; Gerstein, B. C. *J. Appl. Phys.* **1981**, *52*, 5517.
(24) Muruganadam, N.; Koros, W. J.; Paul, D. R. *J. Polym. Sci., Polym. Phys.* **1987**, *25*, 1999.

MA980205G